European Journal of Medicinal Chemistry 82 (2014) 152–163

Contents lists available at ScienceDirect

European Journal of Medicinal Chemistry

journal homepage: http://www.elsevier.com/locate/ejmech

Original article

New mixed ligand zinc(II) complexes based on the antiepileptic drug sodium valproate and bioactive nitrogen-donor ligands. Synthesis, structure and biological properties

Mohanad Darawsheh [a,1], Hijazi Abu Ali [a,*,1], A. Latif Abuhijleh [a], Emilia Rappocciolo [b], Mutaz Akkawi [c], Suhair Jaber [c], Salam Maloul [a], Yasmeen Hussein [b]

[a] Department of Chemistry, Birzeit University, P.O. Box 14, West Bank, Palestine
[b] Department of Biology and Biochemistry, Birzeit University, West Bank, Palestine
[c] Department of Life Sciences, Al-Quds University, West Bank, Palestine

ARTICLE INFO

Article history:
Received 22 July 2013
Received in revised form
7 January 2014
Accepted 13 January 2014
Available online 16 May 2014

Keywords:
Zinc(II) complexes
Nitrogen-based ligands
Valproic acid
Anti-bacterial activity
Anti-malarial activity
Hemozoin
β-Hematin

ABSTRACT

Starting from the precursor [Zinc Valproate complex] (**1**), new mixed ligand zinc(II) complexes of valproic acid and nitrogen-based ligands, formulating as, $[Zn(valp)_2$2,9-dmphen] (**2**), $[Zn_2(valp)_4(quin)_2]$ (**3**), $[Zn(valp)_2(2\text{-ampy})_2]$ (**4**), and $[Zn(valp)_2(2\text{-ampic})_2]$ (**5**) (valp = valproate, 2,9-dmphen = 2,9-dimethyl-1,10-phenanthroline, quin = quinoline, 2-ampy = 2-aminopyridine, 2-ampic = 2-amino-6-picoline) were synthesized and characterized using IR, ^{1}H NMR, $^{13}C\{^1H\}$ NMR and UV–Vis spectrometry. The crystal structures of complexes **2**, **3** and **4** were determined using single-crystal X-ray diffraction. The complexes were also evaluated for their anti-bacterial activity using *in-vitro* agar diffusion method against three Gram-positive (*Micrococcus luteus*, *Staphylococcus aureus*, and *Bacillus subtilis*) and three Gram-negative (*Escherichia coli*, *Klebsiella pneumoniae*, and *Proteus mirabilis*) species. Complex **2** showed considerable activity against all tested microorganisms and the effect of complexation on the anti-bacterial activity of the parent ligand of **2** was also investigated. The anti-bacterial activity of 2,9-dmphen against Gram-negative bacteria was enhanced upon complexation with zinc valproate. On the other hand, complexes **1** and **3** showed weak inhibition activity against the tested species and complexes **4** and **5** didn't show any activity at all. Two methods were used for testing the inhibition of ferriprotoporphyrinIX biomineralization: a semi-quantitative micro-assay and a previously self-developed quantitative *in-vitro* method. Both were used to study the efficiency of these complexes in inhibiting the formation of the Malaria pigment which considered being the target of many known anti-malarial drugs such as Chloroquine and Amodiaquine. Results showed that the efficiency of complex **2** in preventing the formation of β-Hematin was 80%. The efficiency of Amodiaquine as a standard drug was reported to give 91%.

1. Introduction

Zinc, which occurs naturally as divalent cation Zn(II), is one of the most important metal in biological systems as it plays an essential role in the activity of nearly 300 enzymes that catalyze approximately 50 important cellular biochemical reactions [1–3]. In bacteria, Zinc plays a role in catalysis, protein structure and perhaps as a single molecule [4]. However, at high concentrations Zn(II) shows inhibitory action on the growth of bacterial species like *Escherichia coli*, *Staphylococcus faecalis*, *Staphylococcus aureus*, *Staphylococcus epidermidis*, *and Proteus aeruginosa* [5,6].

In some cases, the interaction of metal ions (i.e. Zn(II)) with bioactive anti-bacterial organic compounds increases the biological activity of the ligands [7]. The metal oxidation state, the type and number of donor atoms, as well as their relative positions within the ligand are major factors determining the relationship between the structure and activity. In other cases, the interaction of bioactive organic compounds with metals inhibits their activity, e. g. the anti-bacterial activity of cefadroxil is diminished when it binds to Zn(II) complex [8].

Malaria is a mosquito borne parasitic disease of the blood caused by a Protozoan belonging to the genus Plasmodium. It is considered one of the major public health concerns globally where

* Corresponding author.
E-mail addresses: habuali@birzeit.edu, habuali1@yahoo.com (H. Abu Ali).
[1] Author contributions: These authors are contributed equally to this work.

http://dx.doi.org/10.1016/j.ejmech.2014.01.067
0223-5234/

about 40% of the world's population is currently at risk for malaria disease [9,10]. Plasmodium species have a complex life cycle. During what is known as the intra-erytrhrocytic stage, active metabolism of hemoglobin takes place in an acidic lysosome-like organelle called the food vacuole that has a pH of about (5.0–5.4) [11–14]. Digestion of hemoglobin by malaria parasite leads to the continuous liberation of free heme (Iron protoporphyrin IX) along with oxygen, causing formation of a ferric form of heme called ferriprotoporphyrin IX which can lead to the killing of the parasites. However, Plasmodium parasite has evolved a unique detoxification method of free heme through its conversion into a non-toxic, inert, insoluble, crystalline and black-brown pigment called hemozoin [15].

Hemozoin is made of dimers of hematin molecules that are joined together by hydrogen bonds to form larger structures. These dimers are formed through an iron–oxygen coordinate bond that links the central ferric iron of one hematin to the carboxylate side group oxygen of another [15–18]. These reciprocal ferric-oxygen bonds are highly unusual and have not been observed in any other porphyrin dimer. Antimalarial drugs are believed to act by inhibiting hemozoin formation in the food vacuole. This prevents the detoxification of the free heme released in this compartment, eventually killing the parasite [15,17].

A crystalline synthetic structure known as β-hematin is believed to be structurally, morphology and spectroscopically identical to purified hemozoin [15,19–23]. β-hematin formation could be accomplished in vitro under specific chemical conditions (acidic pH) through a biocrystallization process [24] making it an outstanding target for in vitro screening of antimalarial compounds.

Chloroquine, a quinoline-ring drug, is widely used for malaria treatment. However, resistance to chloroquine has emerged increasing owing to extensive and uncontrolled use [25,26]. Chloroquine resistance is considered as major universal challenging problem and the need of new effective antimalarial drugs is an urge. In this research both a semi-quantitative [27] and a quantitative screening methods for a new potential antimalarial drugs were used [23,24].

Valproic acid (Fig. 1) is a broad spectrum anti-epileptic drug which is effective against all seizure types and is increasingly used in the treatment of other diseases, including bipolar disorder, migraine, and neuropathic pain [28]. In addition, valproic acid was shown to enhance the effect of chemotherapy on EBV-positive tumors, and to possess a multitude of anti-tumor properties *in-vitro* and in clinically relevant animal models [29,30]. Esiobu and Hoosein [31] found that sodium valproate is selectively potent against yeast strains and *Mycobacterium smegmati*. Moreover, synthesis, characterization and biological activity of mixed ligands metal complexes of valproate with different nitrogen based ligands have been studied for copper [32–38], rhodium [39] and platinum [40].

Four bioactive nitrogen base compounds were chosen in the present work: 2,9-dimethyl-1,10-phenanthroline, (2,9-dmphen); quinoline, (quin); 2-aminopyridine, (2-ampy) and 2-amino-6-picoline, (2-ampic). These ligands and their derivatives, as well as many of their complexes, are exhibiting anti-bacterial [41–43], anti-microbial [44–50], anti-fungal [51], anti-viral [52,53] and anti-tumor activities [54–57] which depend on the nature of the ligand and the type of the metal ion.

Zinc complexes of aliphatic carboxylate such as formate, acetate, propionate and butyrate with nitrogen based ligands have been synthesized and screened as bio-active compounds [58–64]. In the present work, we describe the structure and biological activity of mixed ligand zinc valproate complexes with four nitrogen based ligands. The crystal structure, spectroscopic properties, antibacterial and anti-malarial activity of: [Zn(valproate)$_2$2,9-dimethyl-1,10-phenanthroline] (**2**), [Zn$_2$(valproate)$_4$(quinoline)$_2$] (**3**), [Zn(valproate)$_2$(2-aminopyridine)$_2$] (**4**), and [Zn(valproate)$_2$(2-amino-6-picoline)$_2$] (**5**) is reported.

2. Results and discussion

2.1. Synthesis of zinc complexes

Water insoluble white solid, [zinc valproate complex] (**1**), was obtained via the reaction of 1:2 M ratio of $ZnCl_2$ with sodium valproate in water (Scheme 1). A series of novel mixed ligand zinc complexes were prepared by adding N-donor ligands to complex **1**, as shown in Scheme 2. An appropriate molar ratio of the reactants were mixed in methanol and stirred for several hours. The obtained complexes were soluble in methanol and separated from methanol by evaporation. The physical properties of **1**–**5** are summarized in Table S1 (Appendix A. Supplementary Materials).

2.2. Crystallographic studies

2.2.1. X-ray crystal structure determination of [Zn(valp)$_2$2,9-dmphen] (**2**)

The atomic numbering scheme and atom connectivity for complex **2** are shown in Fig. 2 and selected bond lengths and angles are reported in Table 1. Complex **2** crystallizes in *P2*(1)/c space group with four molecules of **2** in the unit cell. The structure consists of monomeric units in which Zn(II) exhibits a highly distorted octahedral geometry in the $ZnN_2O_2 + O_2$ chromospheres. Zn(II) is covalently bonded to two valproate ligands and one bidentate 2,9-dmphen ligand. The mean Zn–N bond distance (2.097 Å) is similar to the same bond in other zinc complexes of 2,9-dmphen ligand; although these complexes exhibit more symmetrical Zn–N distances [66–69].

Each of the valproate groups bond in an asymmetric coordination mode with one of the two valproate oxygens is tightly bonded to Zn (II) {Zn1–O1 = 1.942(2), Zn1–O2 = 2.560; and Zn1–O3 = 2.135(5), Zn1–O4 = 2.324 Å} with the calculated difference between these distances $\Delta_1O = 0.618$ and $\Delta_2O = 0.189$ Å for the two valproate groups, respectively. These distances correspond to Zn–O distance for aliphatic carboxylates [70]. The difference in Zn–O bond distances between the two tightly binding oxygens {Zn1–O1 and Zn1–O3 is significantly large (0.193 Å). This difference is smaller in zinc acetate and zinc isovaleroate complexes {e.g. 0.065 Å in zinc isovaleroate complex} [71–74]. The analysis of C15–O1 and C15–O2 bond distances, 1.260(4) and 1.193(4) Å, respectively, showed that the covalent character of the Zn–O linkage is large, *ca.* 22.8% on the basis of the theory by Hocking and Hambley

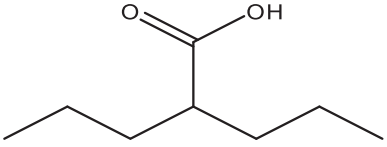

Fig. 1. Structure of valproic acid.

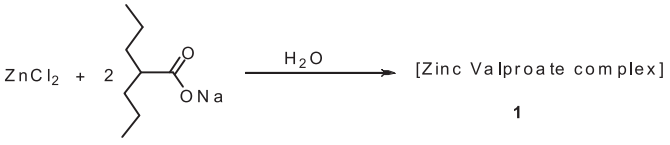

Scheme 1. Synthesis of complex **1**.

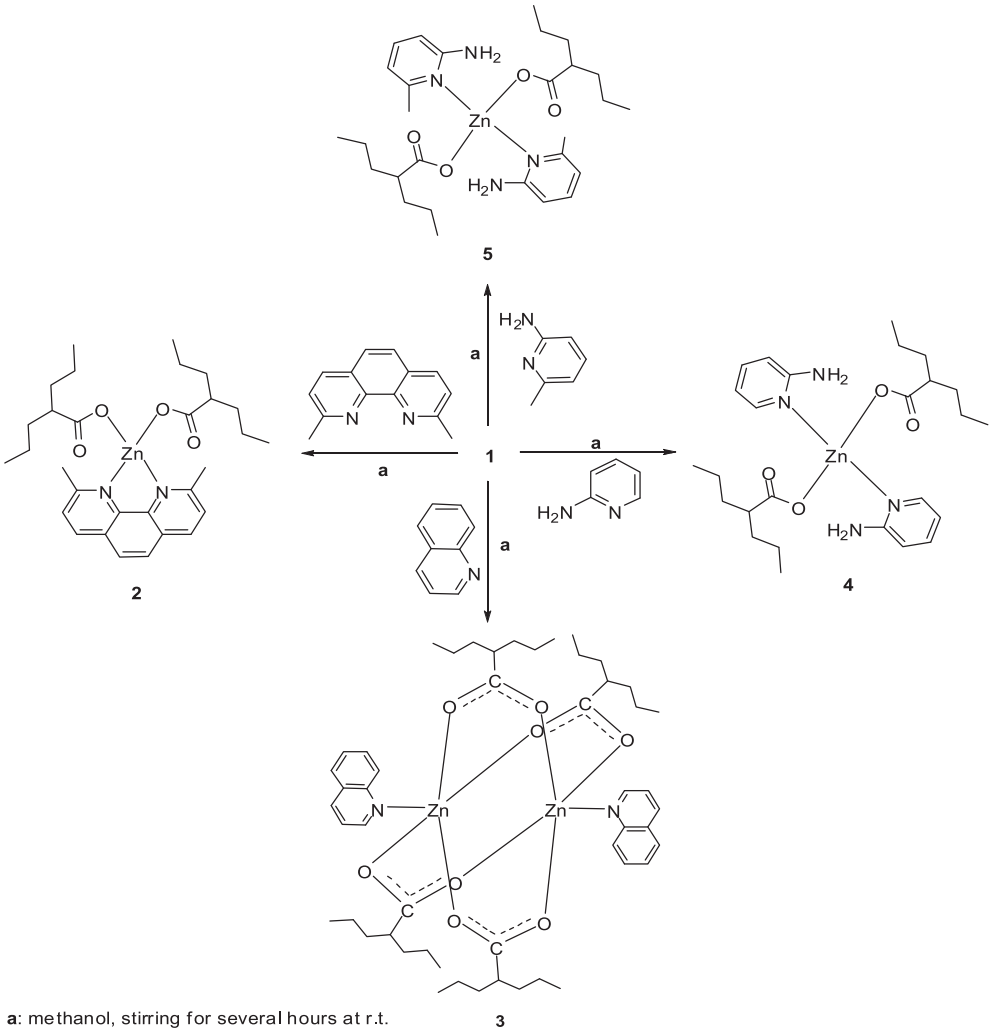

Scheme 2. Synthesis of **2**, **3**, **4** and **5**.

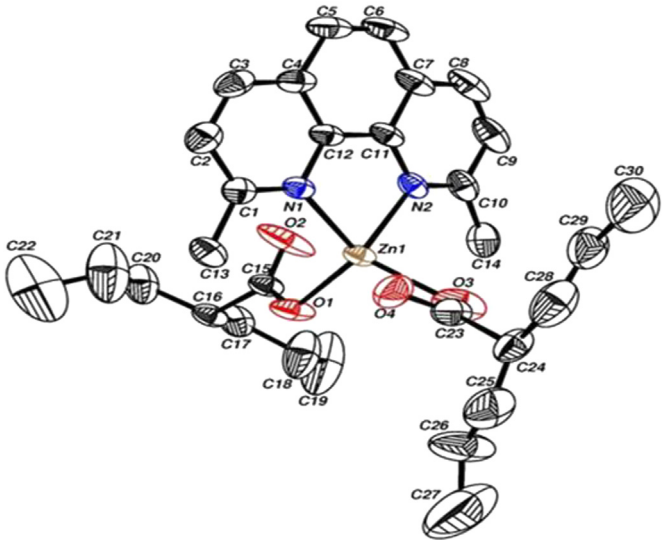

Fig. 2. View of the molecular structure of **2**, showing the atom numbering scheme. Ellipsoids represent thermal displacement parameters at the 50% probability level.

[75]. On the other hand, the covalent character of the second valproate group {C23–O3 = 1.248 Å and C23–O4 = 1.229 Å} is small, *ca*. 6.8% in the basis of the same theory. These results are in agreement with the large difference in the previously discussed Zn–O bond distances.

The basal atomic donor set consists of N1, N2, O1 and O3 atoms with the axial atoms being O2 and O4 with angle of O2–Zn1–O4 = 159.10 (10). The Zn(II) atom exhibits a N_2O_2OO coordination which can be described as a {4 + 1 + 1*} octahedral. The four basal donor atoms are twisted toward a distorted tetrahedron resulted

Table 1
Selected bond distances (Å) and bond angles (°) for **2**.

Distances (Å)		Distances (Å)	
N(1)–Zn(1)	2.108(3)	N(2)–Zn(1)	2.086(3)
O(1)–Zn(1)	1.942(2)	O(3)–Zn(1)	2.135(5)
O(2)–Zn(1)	2.560[a]	O(4)–Zn(1)	2.324[a]
C(15)–O(1)	1.260(4)	C(15)–O(2)	1.193(4)
Angles (°)		Angles (°)	
N(2)–Zn(1)–N(1)	80.76(12)	O(1)–Zn(1)–O(3)	104.04(15)
O(1)–Zn(1)–N(1)	110.09(13)	N(2)–Zn(1)–O(3)	96.10(14)
O(1)–Zn(1)–N(2)	131.18(11)	N(1)–Zn(1)–O(3)	136.94(13)
O(2)–C(15)–O(1)	119.9(3)	O(4)–C(23)–O(3)	118.4(5)

[a] Non-bonded contact distance.

mainly from the differences in ligands (bidentate 2,9-dmphen vs. two monodenate valproate groups). Because of the rigidity of 2,9-dmphen ligand, it forms a fixed five-member ring in which the N1–Zn–N2 angle is constrained to 80.76(12)° but the deformation is also evidence by the other angles of the basal atoms, O1–Zn1–N1 {110.09(13)°}, O3–Zn1–N2 {96.10(14)°} and O1–Zn1–O3 {104.04(15)°} which significantly deviated from the expected square planar angle. The bond distances and angles within the 2,9-dmphen and valproate ligands show the expected values.

2.2.2. Crystal structure of $[Zn_2(valp)_4(quin)_2]$ (**3**)

A view of the molecular structure of complex **3** with numbering scheme is shown in Fig. 3. Selected bond distances and angles for this complex are reported in Table 2.

The structure consists of centro-symmetric binuclear Zn units, which is typical of $[M_2(carboxylate)_4L_2]$ complexes, with the valproate ligands providing the four *syn–syn* metal bridging bidentate carboxylate residues. The valproate ligands display a paddle-wheel-like arrangement about the Zn…Zn axis. Each Zn(II) cation has a square pyramidal coordination geometry with the apex provided by axial coordination of quinoline ligand. Using the geometrical parameter τ ($\tau = |\alpha - \beta|/60$, where α and β are the largest angles around the central atom) defined by Addison and Rao [76]; the analysis of this complex gives a value of 0.005 which suggest the distorted square pyramidal arrangement around Zn(II) atom. The Zn … Zn distance [2.9481(3) Å] for complex **3** is in agreement with the average distance for a four-ligand paddle-wheel Zn_2cluster [2.9–3.0 Å] [77]. There is no evidence or requirement for direct Zn…Zn bonding in this complex.

Zinc to apical atom (N) distance is 2.0556(10) Å which is similar to the average distance of Zn–N in $[Zn(quin)_2Cl_2]$ and $[Zn_2(CH_3CH{=}CHCO_2)_4(quin)_2]$, 2.057(3) and 2.063(2) Å, respectively [78,79]. The Zn–O average distance [2.0460 Å] is in agreement with the value of analogous rhodium complex $[Rh_2(valp)_4(caffeine)_2$,2.041Å] [39], and with the values of structurally characterized paddle-wheel Zn(II) carboxylate complexes which is [2.04 Å] in average [78–83].

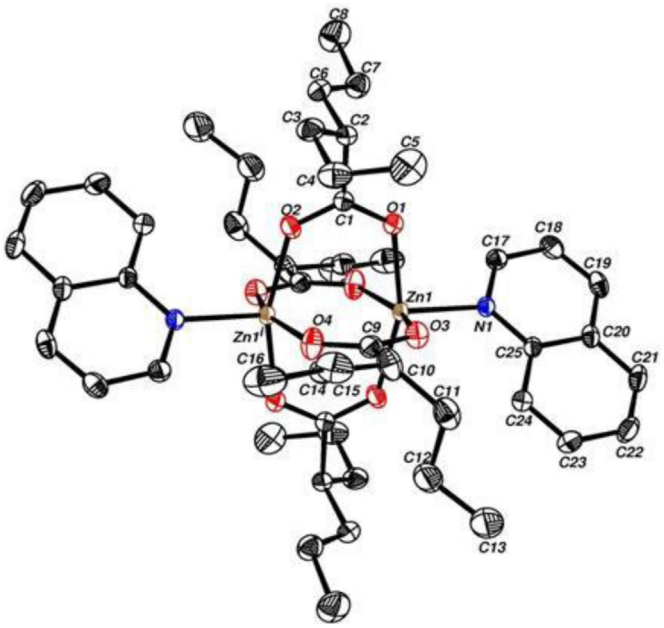

Fig. 3. View of the molecular structure of **3**, showing the atom numbering scheme. Ellipsoids represent thermal displacement parameters at the 50% probability level.

Table 2
Selected bond distances (Å) and bond angles (°) for **3**.

Distances (Å)		Distances (Å)	
Zn(1)–Zn(1[a])	2.9481(3)	Zn(1)–N(1)	2.0556(10)
O(1)–Zn(1)	2.0567(10)	O(2)–Zn(1[a])	2.0343(10)
O(3)–Zn(1)	2.0335(10)	O(4)–Zn(1[a])	2.0593(11)
C(1)–O(1)	1.2515(16)	C(1)–O(2)	1.2544(16)
Angles (°)		Angles (°)	
N(1)–Zn(1)–O(1)	98.93(4)	N(1)–Zn(1)–O(3)	104.11(4)
O(1)–Zn(1)–O(2[a])	159.32(5)	O(1)–Zn(1)–Zn(1[a])	82.23(3)
O(2′)–Zn(1)–O(4[a])	89.31(5)	O(3)–Zn(1)–Zn(1[a])	84.64(3)
N(1)–Zn(1)–Zn(1[a])	171.22(3)	O(2′)–Zn(1)–Zn(1[a])	77.22(3)

[a] Symmetry transformation used to generate equivalent atoms: $-x+1, -y+2, -z$.

The asymmetrical *syn–syn* binding mode of the valproate is demonstrated by the different Zn–O distances with average of [2.0339(10) Å] for Zn1–O3 and Zn1–O2 and [2.0580(10) Å] for Zn1–O1 and Zn1–O4. Moreover, the C–O–Zn angles are different for each valproate with average of 122.8° and 132.4° for the two angles. The C–O distances [C1–O1 = 1.2515(16), C1–O2 = 1.2544(16), C9–O4 = 1.2502(17) and C9–O3 = 1.2573(17) Å] are close in value, which is expected for bridging carboxylates coordination mode.

The M-O-C angles are the most responsive to the change in M…M distance. Therefore, it is expected that Zn–O–C average angle [127.6°] is larger than analogous rhodium complexes [118.8°] [39] which exhibit shorter M…M distance. Koh and Christoph [84], studied a wide range of binuclear tetracarboxylates complexes; they have shown empirically that there is a linear relationship between metal separation and M–M–O angles. The average Zn–Zn–O angle [79.9°] in **3** is in agreement with the empirically predicted value [79.9°] for [2.9481 Å] Zn…Zn separation. Also, the bond distances and angles within quinoline and valproate ligands show the expected values.

2.2.3. X-ray crystal structure determination of $[Zn(Valp)_2(2\text{-}ampy)_2]$ (**4**)

$[Zn(Valp)_2(2\text{-ampy})_2]$ (**4**) exists as a mononuclear complex and crystallized in space group *P6(1)*. A perspective view of complex **4** is shown in Fig. 4 together with the atom labeling scheme used. Selected bond lengths and angles are given in Table 3. The crystal structure consists of discrete molecular species in which zinc form a distorted tetrahedral arrangement, ZnO_2N_2, ligated by N(1) and N(3) of two pyridines and O(1) and O(3) from two valproate groups. Deviation from regular tetrahedral geometry is apparent from observed binding angles, {N1–Zn1–N3 = 102.84(8), O1–Zn1–O3 = 124.92(9), O1–Zn1–N1 = 104.90(9) and O3–Zn1–N3 = 103.12°}, which are significantly deviate from the ideal tetrahedral angle.

The observed bond distances of Zn–N are {2.043(2) and 2.0543(18) Å} for Zn1–N1 and Zn1–N3, respectively, which are slightly longer than the average distance found in $[Zn(2\text{-ampy})_2Cl_2]$ and $[Zn(2\text{-ampy})_2Br_2]$ complexes {2.036 Å} [85,86].

The average Zn–O distance of 1.9423(18) Å is shorter than similar reported distances of aliphatic carboxylates, e.g. {1.974 Å}, {1.973 Å} and {1.957 Å} in $[Zn(acetate)_2(2\text{-ampy})_2]$ [87], $[Zn(acetate)_2(imidazole)_2]$ and $[Zn(propionate)_2(imidazole)_2]$ [88], respectively. In contrast, Zn–O distance in **4** is closer to the value of $Zn(benzoate)_2(2\text{-ampy})_2$ complex {1.930(3) Å} [89], which exhibits similar hydrogen bonding between the amino group and the coordinated oxygen. Due to their monodentate binding mode, the valproate carboxylate groups adopt highly asymmetrical configuration. This resulted in C11–O1 and C19–O3 distances of 1.255(4) and 1.273(2) Å, respectively, for the coordinating oxygen atom

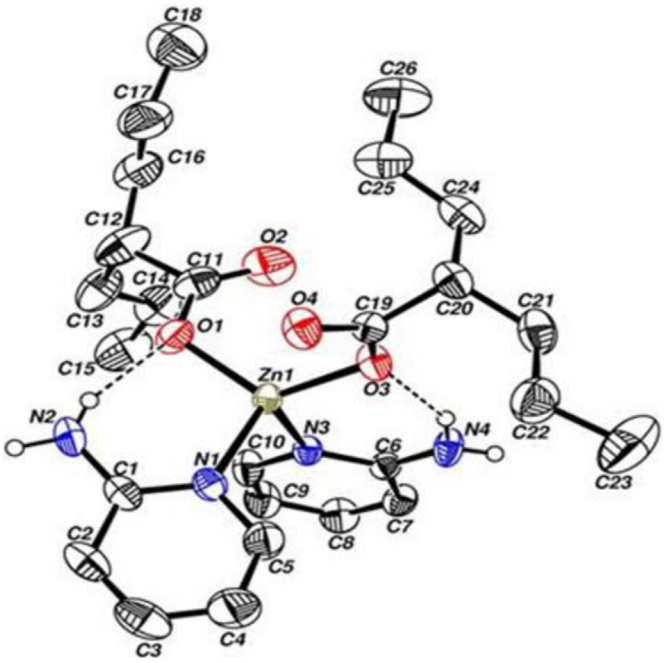

Fig. 4. View of the molecular structure of **4**, showing the atom numbering scheme. Ellipsoids represent thermal displacement parameters at the 30% probability level.

which is clearly longer than non-coordinated oxygen, {1.220(4) and 1.223(3) Å} for C11–O2 and C19–O4 bond distances, respectively. Similar differences were found in other monodentate zinc carboxylate complexes [87–90].

The calculations indicate the presence of intramolecular hydrogen bonding within a molecule and intermolecular hydrogen bonding between molecules (Table 4). The hydrogen bonding between N(2)–H(1N2)…O(1) {2.14(6) Å} and between N(4)–H(1N2)…O(3) {2.10(4) Å} belong to the former (intramolecular), while those between N(2)–H(2N2)…O(2′) {2.01(6) Å}and between N(4)–H(2N4)…O(4′) {2.06(4) Å} belong to the latter (intermolecular). Similar hydrogen bonding exists in Zn(benzoate)$_2$(2-ampy)$_2$ complex [89]. The bond distances and angles within 2-ampy and valproate show the expected values.

2.3. Infrared and U.V–Vis spectra

The magnitude of the difference between the symmetric and asymmetric carboxylate stretching frequencies, [$\Delta = \nu_{as}(COO^-) - \nu_s(COO^-)$], are often used as spectroscopic criteria to determine the mode of carboxylate binding [91,92]. The assignments of IR frequencies for the asymmetric stretch, $\nu_{as}(COO^-)$, the symmetric stretch, $\nu_s(COO^-)$, and the difference between these two values of

Table 3
Selected bond distances (Å) and bond angles (°) for **4**.

Distances (Å)		Distances (Å)	
N(1)–Zn(1)	2.043(2)	N(3)–Zn(1)	2.0543(18)
O(1)–Zn(1)	1.9474(19)	O(3)–Zn(1)	1.9372(17)
O(2)–Zn(1)	2.842[a]	O(4)–Zn(1)	2.903[a]
C(11)–O(1)	1.255(4)	C(11)–O(2)	1.220(4)
Angles (°)		Angles (°)	
N(1)–Zn(1)–N(3)	102.84(8)	O(1)–Zn(1)–O(3)	124.92(9)
O(1)–Zn(1)–N(1)	104.90(9)	O(1)–Zn(1)–N(3)	105.53(8)
O(3)–Zn(1)–N(1)	113.16(8)	O(3)–Zn(1)-N(3)	103.12(7)
O(1)–C(11)–O(2)	122.5(3)	O(3)–C(19)-O(4)	123.1(2)

[a] non-bonded contact distance.

Table 4
Hydrogen-bonding geometry for **4** (Å and °).

N–H…O	d(N–H)	d(H…O)	d(N…O)	<(NHO)
N(2)–H(1N2)....O(1)	0.74(6)	2.14(6)	2.808(4)	152(6)
N(2)–H(2N2)...O(2′)	0.88(6)	2.01(6)	2.877(4)	172(5)
N(4)–H(1N4)...O(3)	0.78(4)	2.10(4)	2.813(3)	151(4)
N(4)–H(2N4)...O(4′)	0.82(4)	2.06(4)	2.860(3)	167(4)

Symmetry transformation used to generate equivalent atoms: (′) y, $-x + y, z - 1/6$, (″) y, $-x + y+1, z - 1/6$.

valproate group in complexes **1**–**5** are given in Table 5. The separation of the frequencies, $\Delta_\nu(COO^-) = 168$ and 175 cm^{-1}, for complexes **1** and **3**, respectively, is an indication of *syn–syn* bridging coordination mode since such zinc complexes usually exhibit $\Delta_\nu(COO^-)$ at 170 ± 10 cm^{-1} [93]. This coordination mode is also confirmed by the single crystal X-ray structure determination of complex **3** (Fig. 3). $\Delta_\nu(COO^-)$ values for copper valproate with bridging coordination carboxylate have been observed at 160 cm^{-1} [33,36,38] which is similar to the $\Delta_\nu(COO^-)$ value of **1**. Three new peaks at 596, 425 and 410 cm^{-1}in the IR spectra of **1** that are not found in sodium valproate could be assigned to Zn–O stretching frequency which occur in this range [94–98].

The large values of $\Delta_\nu(COO^-) = 185$, 221 and 232 cm^{-1} for **2**, **4** and **5**, respectively, indicate a monodentate coordination of the carboxylate groups (see Scheme 2), since [$\Delta_\nu(COO^-)_{2,4,5}$ (185, 221 and 232 cm^{-1}) >> $\Delta_\nu(COO^-)_{Na(valp)}$ (137 cm^{-1})] [91]. This coordination mode is also confirmed by the single crystal X-ray structure determination of complexes **2** and **4** (Figs. 2 and 4).

Complex **4** exhibits two absorptions at 3354 and 3196 cm^{-1} which are assigned to the asymmetrical (ν_{as}(N–H)) and symmetrical (ν_s(N–H)) stretching modes, respectively. Compared to the NH_2 stretching frequencies of 2-ampy ligand [ν_{as}(N–H) = 3447 and ν_s(N–H) = 3185 cm^{-1})], the corresponding peaks of **4** are lowered by [93 cm^{-1}] for ν_{as}(N–H) due to indirect effect of complexation with pyridine nitrogen. The direct complexation with NH_2 will cause larger shift for the two NH_2 peaks [99]. The difference of NH_2 stretching, $\Delta_\nu(NH_2)$, for **4** is 158 cm^{-1}. In contrast, $\Delta_\nu(NH_2)$ for 2-ampy ligand is 262 cm^{-1}, which indicates a strong hydrogen bond formation in complex **4** [99]. The crystal structure of **4** confirmed the hydrogen bonding between the hydrogen of the amino group and the oxygen atom of valproate (see Section 2.2.3). Similar results have been observed for **5** which suggest a similar structure of **4** [for **5**: ν_{as}(N–H) = 3315 cm^{-1}, ν_s(N–H) = 3162 cm^{-1} and $\Delta_\nu(NH_2)$ = 153 cm^{-1}, for 2-ampic: ν_{as}(N–H) = 3461 cm^{-1}, ν_s(N–H) = 3171 cm^{-1} and $\Delta_\nu(NH_2)$ = 290 cm^{-1}].

Absorption spectra of all complexes (**1**–**5**) were performed in DMSO and were very similar to those of the parent N-donor ligands with only 1–5 nm shift caused by the coordination to zinc (Table 5). Thus all bands of the complexes are based to ligands. The spectra are also similar to zinc chloride complexes of the N-donor ligands (unpublished data).

Table 5
UV–Visible and IR spectral data for the complexes.

Assignments	1	2	3	4	5	Na(valp)
$\nu_{as}(COO^-)$ (cm^{-1})	1594	1596	1595	1613	1616	1548
$\nu_s(COO^-)$ (cm^{-1})	1426	1411	1420	1392	1384	1411
$\Delta_\nu(COO^-)$ (cm^{-1})	168	185	175	221	232	137
λ_{max} (nm)	–	271	271	300	300	–
		300 (sh)	315			
		330 (sh)				

*(sh) = shoulder.

Table 6
$^{13}C\{^1H\}$ NMR spectral data of selected carbons for **1**–**5** and there parent ligands.[a]

Compound	COO^-	γ-Carbon[b]	α-Carbon[b]
1	186.03		
2	184.19	138.82	160.59
3	185.229	137.60	150.48
4	184.07	139.51	146.51
5	–[c]	138.90	156.12
NaValp	186.70		
2,9-dmphen		136.23	159.20
Quinoline		135.90	150.26
2-ampy		137.66	158.85
2-ampic		137.99	156.66

[a] ppm downfield relative to TMS as internal standard ($CDCl_3$). For detailed data and references see Tables S2–S6.
[b] See Figure S1.
[c] Not observed.

2.4. ^1H and $^{13}C\{^1H\}$ NMR

The ^1H and $^{13}C\{^1H\}$ NMR spectral data for complex **1**, sodium valproate and valproic acid are reported in Table S2 (Appendix A. Supplementary Materials). Comparison of the ^1H NMR spectra of **1** and sodium valproate showed a downfield shift of the former due to complex formation. This deshielding effect may be due to electron donation of the carboxylate group to the zinc ion. The NMR data of **1** is similar to those observed for rhodium and platinum valproate complexes [39,40]. The ^1H and $^{13}C\{^1H\}$ NMR spectral data for **2**–**5** and their parent N-donor ligands are reported in Tables S3–S6 (Appendix A. Supplementary Materials). The results are in agreement with the proposed structures shown in Scheme 2. The ^1H NMR chemical shifts of the N-donor ligands of **2**–**5** were found in the expected positions of free ligands with almost all protons showing a slightly broad downfield shift, which provide evidence for coordination of ligands to zinc metal through the nitrogen atom.

The $^{13}C\{^1H\}$ NMR chemical shift of carbonyl (COO^-) group depends on the coordination mode and the coordination number of metal ions [100,101]. The chemical shifts of (COO^-) in metal carboxylates are in the following order: bidentate chelating > bidentate bridging > monodentate. The value of $\delta^{13}C$ chemical shift of carbonyl group in complexes **1**–**5** are in agreement with this order (Table 6), since complexes **1** and **3** with bridging carboxylate coordination showed higher $\delta^{13}C$ (COO^-) chemical shift [186.03 and 185.23 ppm, respectively] than the monodentate complexes **2** and **4** with $\delta^{13}C$ (COO^-) chemical shift of 184.19 and 184.07 ppm, respectively. However, the $\delta^{13}C$ (COO^-) signal was absent in complex **5**.

In general, the γ-carbon atom of pyridine derivatives (see Fig. S1) is the appropriate position to study the $^{13}C\{^1H\}$ NMR chemical shift in order to investigate the metal-pyridine coordination bond. The γ-carbon atom lies on the same symmetry axes and planes of the nitrogen atom and is the most distant atom from the nitrogen atom so that anisotropic and local effects are apparently attenuated [102].

The γ-carbon atom of the N-based ligands of all complexes **2**–**5** exhibit downfield chemical shift in the range of 0.9–2.9 ppm from the free ligand value, supporting complex formation (see Table 6) which is explained by the depletion of electron density caused by bond formation with pyridine nitrogen atom [103]. On the other hand, the α-carbon atoms of the pyridine derivatives (see Figure S1, Appendix A. Supplementary Materials) of almost all complexes **2**–**5** exhibit upfield shift (or at least very small downfield shift) compared to those of free ligands (Table 6). Apparently, this effect is caused by a change in the electron distribution about the α-carbon rather than the net electron density. The polarization of electron density from the nitrogen atom toward the metal causes a polarization of electron density from α-carbon which, in turn, is compensated for through inductive effect toward the α-carbon from the β-carbon. The net effect is anisotropic with respect to the α-carbon irrespective of the total electron density about this center. Such an effect is not found for the α-hydrogen atom [103,104].

2.5. Anti-bacterial activity

Before we performed the biological measurements the solution stability of the complexes **1**–**5** was checked periodically by ^1H and ^{13}C NMR spectroscopy in chloroform and DMSO solvents and always obtained the same data. In addition, the complexes were crystallized by solvent evaporation which took several days and the NMR measurements were repeated to give the same physical properties of the compounds.

Zinc valproate complexes **1**–**5** have been evaluated *in-vitro* against three Gram-positive (*Micrococcus luteus*, *S. aureus*, *Bacillus subtilis*), and three Gram-negative (*E. coli*, *Klebsiella pneumoniae* and *Proteus mirabilis*) bacteria species. The results (Table 7) were obtained by the well-diffusion method using a 10 mmol/L concentration (in DMSO) with a volume of 50 μL per well.

Complex **1** showed anti-bacterial activity against all tested microorganisms except for *P. mirabilis* with inhibition zone diameter (IZD) ranging between 8 and 13 mm. Complex **2** showed good anti-bacterial activity against Gram-positive bacteria with IZD ranging between 18 and 23 mm. For the Gram-negative bacteria complex **2** showed weaker inhibition activity with IZD ranging between 8 and 12 mm. Complex **3** showed anti-bacterial activities against all tested microorganisms with IZD ranging between 7 and 15 mm. Complexes **4** and **5** did not show anti-bacterial activity against any of the tested microorganisms. The parent ligand sodium valproate (tested twice as water and DMSO solution) and zinc ion (as $ZnCl_2$) did not show anti-bacterial activity against any of the tested microorganisms at 10 mmol/L concentration.

Three different solutions with two fold decreasing concentration, 10, 5 and 2.5 mmol/L of the complexes **1**, **2** and **3** and their parent N-donor ligands were tested against the same six bacterial species mentioned above. Also the minimum inhibition concentration (MIC) was determined for complexes **1**, **2** and **3** and their parent ligands. The data are listed in Table 8. The results obtained for complexes **1** and **3** demonstrate the similarity of anti-bacterial activity of the two compounds. The anti-bacterial activity against *M. luteus*, *S. aureus* and *E. coli* have been shown to possess moderate to weak activity at 10 and 5 mmol/L concentrations and is almost absent at 2.5 mmol/L concentration (8 mm for **3** against *S. aureus* and for **1** against *M. luteus* was considered as very weak inhibition). For the other bacteria the inhibition activity was absent at 5 mmol/L concentration. The parent ligands valproate and quinoline did not show anti-bacterial activity at 10 mmol/L. The results of **1** and **3** indicated that the increase of anti-bacterial activity was due to complexation compared to their valproate parent ligands.

Complex **2** showed higher anti-bacterial activity against the investigated Gram-positive bacteria (*M. luteus*, *S. aureus* and *B. subtilis*) compared to Gram-negative bacteria (*E. coli*, *K. Pneumoniae*, *P. mirabilis*). The anti-bacterial activity of complex **2** was not significantly affected by concentration. The parent ligand 2,9-dmphen showed slightly higher anti-bacterial activity than complex **2** against the Gram-positive bacteria. On the other hand, the complexation of 2,9-dmphen with zinc valproate enhanced the anti-bacterial activity against Gram-negative bacteria at all concentrations; 2,9-dmphen ligand did not show anti-bacterial activity against *E. coli* and *P. mirabilis* and the MIC value of 2,9-dmphen against *K. pneumoniae* was 5 mmol/L and in contrast, complex **2** showed activity against the Gram-negative bacteria, *E. coli*,

Table 7
In-vitro anti-bacterial activity data of complexes **1**–**5**.

Diameter of zones showing complete inhibition of growth (mm)[a]						
Compound	*M. luteus*	*S. aureus*	*B. subtilis*	*E. coli*	*K. pneumoniae*	*P. mirabilis*
1	12.7 ± 1.2	11.4 ± 1.3	8.6 ± 1.1	9.0 ± 1.0	10.3 ± 1.5	–
2	18.0 ± 1.8	22.6 ± 1.1	19.7 ± 0. 6	11.0 ± 1.4	12.0 ± 1.0	8.4 ± 0.6
3	13.0 ± 0.8	15.3 ± 1.0	11.0 ± 1.0	10.5 ± 0.7	11.0 ± 1.6	7.7 ± 1.2
4	–	–	–	–	–	–
5	–	–	–	–	–	–
valp	–	–	–	–	–	–
$ZnCl_2$	–	–	–	–	–	–

- dashes indicated zero inhibition, all microorganisms were resistant to DMSO.
[a] The data stated as average ± standard deviation ($N = 3$), the concentration was 10 mmol/L in DMSO.

K. pneumoniae and *P. mirabilis*, with MIC values 0.6, 2.0 and 2.5 mmol/L, respectively.

The anti-bacterial activity of 2,9-dmphen and their metal complexes have been studied very well [41,42,44,105,106]. The present study showed that the complexation of 2,9-dmphen enhanced the activity against Gram-negative bacteria and did not affect the activity against Gram-positive bacteria. This difference could be explained by the different cell wall structure of Gram-positive and Gram-negative bacteria. It is possible that the enhancement of lipophilicity of complex **2** plays a role in the increased activity.

2.6. Anti-malarial activity

2.6.1. Semi-quantitative method

Two different zinc valporate complexes, complex **2** and complex **A** {zinc(valp)$_2$(1,10-phenanthroline)(H_2O), see reference [107]}, and their parent phenanthroline derivative ligands were all evaluated for their inhibitory effect on *in-vitro* beta-hematin formation. Results of the semi-quantitative method are shown in Fig. 5 and Fig. 6.

Table 8
In-vitro anti-bacterial activity data at different concentrations and the MIC values of complexes **1**–**3** and their parent ligands.

Diameter of zones showing complete inhibition of growth (mm)[a]						
	M. luteus	*S. aureus*	*B. subtilis*	*E. coli*	*K. pneumoniae*	*P. mirabilis*
Complex 1[b]						
10	12	11	9	9	10	–
5	10	9	–	7	–	–
2.5	8	–	–	–	–	–
MIC	2.5	5	10	5	10	>10
Complex 2						
10	19	22	20	11	12	9
5	17	20	19	10	10	8
2.5	14	19	18	9	8	7
MIC	0.8	0.2	0.2	0.6	2	2.5
2,9-dmphen						
10	20	25	22	–	9	–
5	18	22	20	–	7	–
2.5	12	20	16	–	–	–
MIC	1.5	0.2	0.2	>10	5	>10
Complex3						
10	12	14	12	10	9	7
5	8	11	7	9	–	–
2.5	–	8	–	–	–	–
MIC	5	2.5	5	5	10	10

[a] The data are the rounded average of two trials, - dashes indicated zero inhibition, all microorganisms were resistant to DMSO. The parent ligands valproate and quinoline did not show antibacterial activity at 10 mmol/L.MIC values are in mmol/L and>10 mean that this complex is not active at the highest tested concentration (10 mmol/L).
[b] Three different concentrations 10, 5 and 2.5 mmol/L in DMSO. MIC: minimum inhibition concentration.

On the other hand, complexes 3, 4 and 5 did not show any significant inhibitory activity on *in-vitro* beta-hematin formation.

As shown in Fig. 5, the absorbance value of each of the four tested compounds were measured at 405 nm and compared to three positive controls (CQ, AQ and 2-MP) and two negative controls (water and DMSO). Complex **2**, with an absorbance value of 0.076 (at a concentration of 1 mg/ml) was the only one of these four compounds with a potential anti-malarial activity when compared to the standard drugs (at a concentration of 0.1 mg/ml). The efficiency of the drug used is inversely proportional to the absorption, low absorption indicates higher efficiency and vice versa. It is important to mention that each result is the average of 26 individual experiments. It is obvious that complex **2** needs more investigation and the test was repeated using lower concentrations of this complex. Different dilutions of complex **2** were made and results are summarized in Fig. 6. Complex **2** with the range of concentrations between 1 and 0.7 mg/ml showed a good inhibition activity on the formation of β-hematin.

2.6.2. Quantitative method

According to method of use, the result of complex compared to DMSO (as negative control) and Amodiaquine (AQ as positive control) in terms of β-Hematin formation is shown in Fig. 7. Comparison in terms of drug efficiency is seen in Fig. 8.

Fig. 7 represents the percentage yield of β-Hematin formation. Interestingly, the percentage yield of β-hematin formation in the presence of complex **2** was 20% and that of AQ was 9%, both at concentration 0.4 mM comparing to the negative control which was 83%.

Comparison in terms of efficiency of the complex under investigation as anti-malarial drug is shown in Fig. 8. It is obvious that complex **2** has a considerable anti-malarial activity in inhibiting β-hematin formation with efficiency 80%, when compared to CQ 91%, and DMSO 17%.

This inhibition activity of β-hematin may be due to the interactions between complex **2** and ferri-heme; which inhibited the formation of β-hematin in vitro. Forces involved in stability of this interactions may involved π-π stacking forces of the phenanthroline ring over the porphyrin, hydrogen bonding interaction between valproate oxygen atoms and propanoic acid of the ferri-heme and coordination bond between zinc(II) and the N-donor groups of the heme [108].

Complex **A** (see Fig. 5) did not show any considerable activity although it's similar to complex **2**. These two complexes are different in the methyl groups in the 1 and 9 positions of the phenanthroline in complex **2** and the coordination number around zinc (II) since complex **A** contains additional H_2O groups that coordinate to zinc. So may be the free coordination site on zinc (II) in complex **2** plays a major rule in stabilizing the interaction with ferri-heme. The additional methyl groups of the 2,9-**dimethyl**-1,10-phenanthroline may

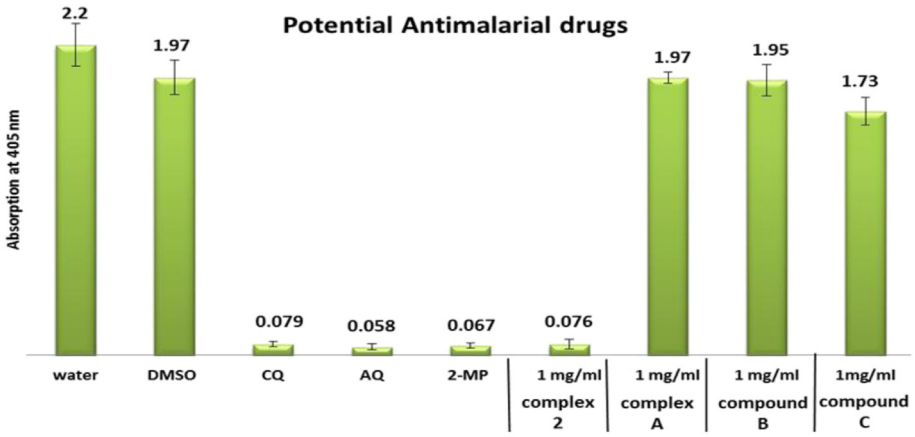

Fig. 5. Column diagram representing Semi-Quantitative test results of potential anti-malarial drugs. Complex **2** = Zn (valp)$_2$–2,9-dimethyl-1,10-phenanthroline, complex **A** = Zn(valp)$_2$(1,10-phenanthroline)(H_2O) [107], compound **B** = 1,10-phenanthroline and compound **C** = 2,9 dimethyl-1,10-phenanthroline compared to Chloroquine (CQ), Amodiaquine (AQ) and 2-mercaptopyrmidine (2-MP) as positive controls (0.1 mg/ml) while water and DMSO used as negative controls. Absorption is inversely proportional to drugs efficiency, the lower the absorption is, the drug is considered to be more efficient.

also form electrostatic interaction with ferri-heme. Either way the mechanism of inhibition is thought to be through the formation of a complex between complex **2** and ferriheme which prevent the formation of β-hematin.

3. Conclusion

X-ray crystallography, ^{1}H NMR, ^{13}C{^{1}H} NMR, Infrared and UV–Vis spectrometric techniques were used to study and characterize new mixed ligand complexes of zinc valproate with N-donor heterocyclic ligands. The synthesized complexes were [Zn$_2$(valp)$_4$] (**1**), [Zn(valp)$_2$2,9-dmphen] (**2**), [Zn2(valp)$_2$(quin)$_2$] (**3**), [Zn(valp)$_2$(2-ampy)$_2$] (**4**) and [Zn(valp)$_2$(2-ampic)$_2$] (**5**).

All compounds showed anti-bacterial activity against different Gram-positive and Gram-negative bacteria except complexes **4** and **5**. The complexes **1** and **3** have shown higher anti-bacterial activity than their parent valproate ligand. Complex **2** showed higher anti-bacterial activity against Gram-negative bacteria than 2,9-dmphen ligand. For Gram-positive bacteria the activity of **2** and 2,9-dmphen are similar.

Complex **2** showed a very good inhibition activity on the formation of the β-hematin. It should be illustrated that ongoing research will be carried out in our laboratory to study the toxicity and the *in-vivo* effects of this compound to gain a further understanding of their biological action.

Valproic acid was used clinically as anti-convulsant drug, primarily in the treatment of epilepsy and bipolar disorder. Also it appears to have wide implications in the treatment of various cancer types. Therefore, further work may include other biological activity applications of these complexes as anti-convulsant and anti-cancer agents.

4. Experimental

4.1. Chemicals, materials and biological species

Zinc(II) chloride was purchased from Merck, sodium valproate was purchased from Sigma, 2,9-dimehtyl-1,10-phenanthroline,quinoline, 2-aminopyridine and 2-amino-6-picoline were purchased from Aldrich. All solvents used were of analytical reagent grade and purchased from commercial sources. *M. luteus*, *S. aureus*, *B. subtilis*, *E. coli*, *Klebsiella pneumonia* and *P. mirabilis* were kindly obtained from Biology and Biochemistry Department at Birzeit University.

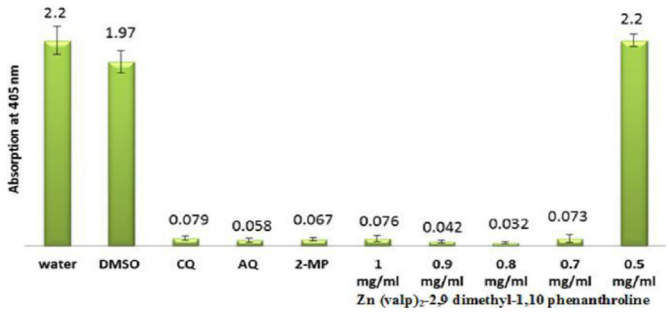

Fig. 6. Column diagram representing the efficiency of the complex **2** (Zn (valp)$_2$–2,9 dimethyl-1,10 phenanthroline) compared to the negative and positive controls (Chloroquine(CQ), Amodiaquine(AQ) and 2-mercaptopyrimidine (2-MP) at 0.1 mg/ml), showing the absorption values of dissolved β-Hematin (alkaline hematin) at 405 nm using ELISA reader, according to E. Deharo semi-quantitative method [27]. The absorption is inversely proportional to drugs efficiency, the lower the absorption is, the drug is considered to be more efficient.

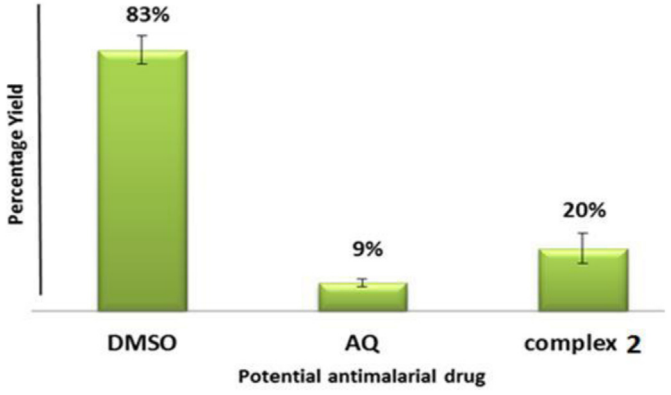

Fig. 7. Column diagram representing the percentage yields of potential anti-malarial drug complex **2** (Zn (valp)$_2$–2,9- dimethyl-1,10 phenanthroline) compared to Amodiaquine and DMSO at 0.4 mM. Yields are inversely proportional to drugs efficiency, the lower the yield is, the drug is considered to be more efficient.

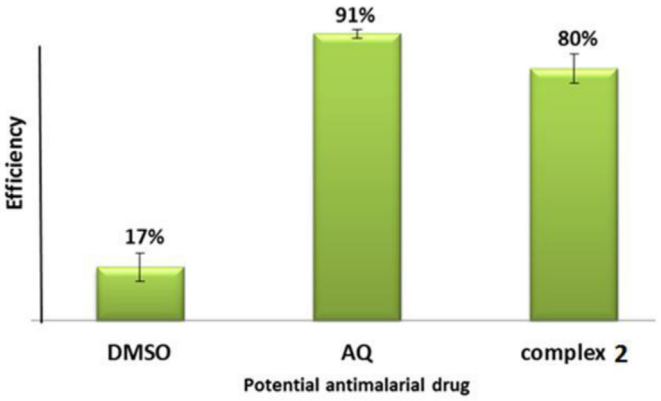

Fig. 8. Column diagram representing the efficiency of potential anti-malarial drug, complex **2** (Zn $(valp)_2$-2,9- dimethyl-1,10 phenanthroline) compared to Amodiaquine and water, all at a concentration of 0.4 mM.

4.2. Physical measurements

Infrared (IR) spectra were recorded in the 200–4000 cm^{-1} region (KBr) on a Varian 600 FT-IR Spectrometer. UV–Vis spectra were recorded using Hewlett Packard 8453 photo diode array spectrophotometer in the 200–800 nm region using DMSO as solvent. NMR spectra were recorded on a Varian Unity Spectrometer operating at 300 MHz for ^1H measurements and 75 MHz for the $^{13}C\{^1H\}$ measurements. Melting points were determined in capillary tubes with EZ-Melt apparatus without any correction.

4.3. Synthesis of Zn(II) complexes

The synthesis of all zinc(II) complexes was conducted at room temperature in ambient conditions.

4.3.1. Synthesis of [zinc valproate complex] (*1*)

Water solution of sodium valproate was gradually added to a stirred aqueous solution of zinc chloride in 2:1 M ratio and immediate white solid was formed. The solid was filtered off, washed with cold water and allowed to stand for air drying. The compound is soluble in methanol, ethanol, acetone, chloroform, dichloromethane, diethyl ether and ethyl acetate [107].

[Zinc valproate complex] (1): ~88% yield, m.p. (>250) °C. ^1H NMR ($CDCl_3$): δ (ppm) 0.87 (t, 6H, CH_3, $^3J_{H\text{-}H} = 7.2$ Hz), 1.24–1.44 (m, 6H, CH_2), 1.56 (m, 2H, CH_2), 2.39 (m, 1H, CH). $^{13}C\{^1H\}$ NMR ($CDCl_3$): δ (ppm) 14.16 (CH_3), 20.64 (CH_2), 35.05 (CH_2), 47.72 (CH), 186.03 (C=O). IR (KBr, cm^{-1}): 2956 s, 2930 s, 2870 m, 1594 vs, 1450 s, 1426 vs, 1328 s, 1229 s, 1120 s, 1067 w, 984 w, 940 w, 874 m, 757 m, 685 m, 663 m, 596 w, 524 m, 475 w, 425 w, 410 w.

4.3.2. Synthesis of [Zn$(valp)_2$2,9-dmphen] (*2*)

2,9-Dmphen (0.92 g, 4.4 mmol) was dissolved in methanol and gradually added to stirred methanol solution of complex **(1)** (1.55 g, 2.2 mmol). The solution was stirred for several hours then evaporated to get a solid residue. The solid product was collected then washed with ether and allowed to dry in air. Suitable crystals for X-ray structural analysis were obtained by recrystallization from acetone. The compound is soluble in methanol, ethanol, dichloromethane chloroform and acetone.

[Zn$(valp)_2$2,9-dmphen] (2): 84% (2.07 g) yield, m.p. (182–187) °C. ^1H NMR ($CDCl_3$): δ (ppm) 0.81 (t, 12H, $CH_{3(valp)}$, $^3J_{H\text{-}H} = 7.4$ Hz), 1.21–1.38 (m, 12H, CH_2), 1.53 (m, 4H, CH_2), 2.34 (m, 2H, $CH_{(valp)}$), 3.12 (s, 6H, CH_3), 7.69 (d, 2H, CH, $^3J_{H\text{-}H} = 8.4$ Hz), 7.84 (ds, 2H, CH, $^4J_{H\text{-}H} = 0.9$ Hz), 8.35 (d, 2H, CH, $^3J_{H\text{-}H} = 8.4$ Hz). $^{13}C\{^1H\}$ NMR ($CDCl_3$): δ (ppm) 14.29 ($CH_{3(valp)}$), 20.90 (CH_2), 24.95 (CH_3), 35.53 (CH_2), 46.63 ($CH_{(valp)}$), 125.63 (CH), 126.15 (CH), 127.03 (C), 138.82 (CH), 140.52 (C–N), 160.59 (**C**–CH_3), 184.19 (C=O). IR (KBr, cm^{-1}): 3050 vw, 3020 vw, 2960 s, 2929 s, 2869 m, 1618 s, 1596 vs, 1569 s, 1504 s, 1453 s, 1411 vs, 1360 w, 1310 m, 1272 m, 1221 m, 1151 w,

Table 9
Crystal data and structure refinement for **2**–**4**.

	2	**3**	**4**
Formula	$C_{30}H_{42}N_2O_4Zn$	$C_{50}H_{74}N_2O_8Zn_2$	$C_{26}H_{42}N_4O_4Zn$
F.W.	560.03	961.86	540.01
Temp, K	173(1)	173(1)	173(1)
Radiation	Mo Kα, 0.71073 Å	Mo Kα, 0.71073 Å	Mo Kα, 0.71073 Å
Cryst size, mm^3	0.36 × 0.30 × 0.28	0.40 × 0.36 × 0.24	0.32 × 0.30 × 0.20
Cryst system	Monoclinic	Monoclinic	Hexagonal
Space group	P2(1)/c	P2(1)/n	P6(1)
a, Å	14.115(3)	11.1032(7)	15.6539(4)
b, Å	22.460(5)	15.712(1)	15.6539(4)
c, Å	9.479(2)	14.1570(9)	20.792(1)
α, deg	90	90	90
β, deg	96.795(3)	91.440(1)	90
γ, deg	90	90	120
V, $Å^3$	2984(1)	2469.0(3)	4412.5(3)
Z	4	4	6
*d*calcd, g cm^{-3}	1.247	1.294	1.219
F(000)	1192	1024	1728
μ, mm^{-1}	0.858	1.024	0.869
θ range, deg .	2.32 to 27.00	2.36 to 28.04	2.47 to 28.00
Reflections collected	32379	27778	50876
Independent reflections	6486 [R(int) = 0.0293]	5886 [R(int) = 0.0211]	7086 [R(int) = 0.0348]
hkl limits	−18,18/−28,28/−12,12	−14,14/−20,20/−18,18	−20,20/−20,20/−27,27
Completeness to theta = 28.00°	99.7% (27.00°)	98.4%	99.9%
Absorption correction	None	None	None
Max. and min. transmission	None	None	None
Refinement method	Full-matrix least-squares on F^2	Full-matrix least-squares on F^2	Full-matrix least-squares on F^2
Data/restraints/parameters	6486/3/340	5886/4/312	7086/1/332
Goodness-of-fit on F^2	1.070	1.047	1.048
Final *R* indices[a] [*I* > 2sigma(I)]	*R*1 = 0.0680, wR2 = 0.1880	*R*1 = 0.0275, wR2 = 0.0727	*R*1 = 0.0380, wR2 = 0.0934
R indices (all data)	*R*1 = 0.0784, w*R*2 = 0.1960	*R*1 = 0.0304, w*R*2 = 0.0745	*R*1 = 0.0432, w*R*2 = 0.0966
Largest diff. peak and hole	1.017and −0.549 e.$Å^{-3}$	0.364 and −0.218	0.752 and −0.258 e.$Å^{-3}$

[a] $RI = \sum||F_o| - |F_c||/\sum F_o$ and.$wR2 = \{\sum[w(F_0^2 - F_c^2)^2]/\sum[w(F_0^2)^2]\}^{1/2}$.

1115 w, 1036 w, 941 w, 865 s, 778 m, 758 m, 734 m, 680 w, 657 m, 582 w, 550 w, 430 w, 413 w. UV–Vis (DMSO, λ (nm)): 271, 300 (sh), 330 (sh).

4.3.3. Synthesis of $[Zn_2(valp)_4(quin)_2]$ (3)

Quinoline (0.91 mL, 0.99 g, 7.7 mmol) was added to a stirred methanol solution of complex (**1**) (1.34 g, 1.9 mmol). The solution was stirred for several hours then concentrated under vacuum and allowed to stand at room temperature. Needle-like crystals were deposited over a period of several days. The crystals were collected and air-dried. For a preparative aspect, quinoline (0.34 mL, 0.37 g, 2.9 mmol) was added to stirred solution of $[Zn_2(valp)_4]$ (**1**) (1.00 g, 1.4 mmol) in methanol. The solution was then stirred for several hours and left to stand for evaporation. The oily product was washed with petroleum ether to give a solid which was allowed to air-dry. The compound was soluble in methanol, ethanol, chloroform and acetone.

$[Zn_2(valp)_4(quin)_2]$ (**3**): 82% (1.10 g) yield, m.p. (66–72) °C. ^{1}H NMR ($CDCl_3$): δ (ppm) 0.883 (t, 12H, CH_3, $^3J_{H\text{-}H}$ = 7.5 Hz), 1.315 (m, 8H, CH_2), 1.401 (m, 4H, CH_2), 1.594 (m, 4H, CH_2), 2.426 (m, 2H, $CH_{(valp)}$), 7.486 (d, d, 1H, CH, $^3J_{H\text{-}H}$ = 4.2), 7.608 (t, 1H, CH, $^3J_{H\text{-}H}$ = 7.0 Hz), 7.767 (t, 1H, CH, $^3J_{H\text{-}H}$ = 7.0 Hz), 7.876 (d, 1H, CH, $^3J_{H\text{-}H}$ = 8.5 Hz), 8.209 (d, 1H, CH, $^3J_{H\text{-}H}$ = 8.5 Hz), 8.266 (d, 1H, CH, $^3J_{H\text{-}H}$ = 7.5 Hz), 8.991 (d, 1H, CH, $^3J_{H\text{-}H}$ = 3.5 Hz). ^{13}C{^{1}H} NMR ($CDCl_3$): δ (ppm) 14.095 (CH_3), 20.397 (CH_2), 35.172 (CH_2), 47.376 ($CH_{(valp)}$), 121.185 (CH), 126.900 (CH), 127.049 (CH), 127.941 (CH), 128.527 (C), 130.162 (CH), 137.603 (CH), 147.221 (C), 150.478 (CH), 185.229 (C=O). IR (KBr, cm^{-1}): 3075 vw, 3035 vw, 3010 vw, 2957 s, 2932 s, 2870 m, 1620 s, 1595 s, 1588 s, 1511 m, 1454 s, 1420 s, 1377 m, 1318 m, 1240 w, 1200 w, 1116 w, 1052 w, 955 w, 856 w, 807 s, 782 s, 750 w, 737 m, 635 w, 588 w, 528 w, 488 w, 466 w. UV–Vis (DMSO, λ (nm)): 271, 315.

4.3.4. Synthesis of [Zn (valp)$_2$(2-ampy)$_2$] (4)

Same procedure was followed as in compound **2** except with 2-ampy (0.96 g, 10.2 mmol) and complex (**1**) (1.80 g, 2.6 mmol). Suitable crystals for X-ray structural analysis were obtained by recrystallization from 1:1 mixture of chloroform and dichloromethane. The compound is soluble in methanol, dichloromethane, chloroform and acetone.

$[Zn(valp)_2(2\text{-}ampy)_2]$ (**4**): 63% (1.75 g) yield, m.p. (126–130) °C. ^{1}H NMR ($CDCl_3$): δ (ppm) 0.84 (t, 6H, CH_3, $^3J_{H\text{-}H}$ = 7.2 Hz), 1.19–1.42 (m, 6H, CH_2), 1.56 (m, 2H, CH_2), 2.38 (m, 1H, $CH_{(valp)}$), 6.00 (bs, 2H, NH_2), 6.52 (m, 2H, CH), 7.40 (t, 1H, CH, $^3J_{H\text{-}H}$ = 7.0 Hz), 7.89 (d, 1H, CH, $^3J_{H\text{-}H}$ = 3.6 Hz). ^{13}C{^{1}H} NMR ($CDCl_3$): δ (ppm) 14.51 (CH_3), 21.03 (CH_2), 35.74 (CH_2), 47.21 ($CH_{(valp)}$), 111.37 (CH), 113.04 (CH), 139.51 (CH), 146.51 (CH), 159.47 (C–NH_2), 184.072 (C=O). IR (KBr, cm^{-1}): 3354 s, 3196 s, 2956 s, 2930 s, 2870 m, 1663 s, 1613 vs, 1568 s, 1501 vs, 1454 s, 1392 s, 1341 m, 1272 s, 1221 m, 1162 m, 1112 m, 1007 s, 932 w, 851 m, 771 vs, 744 w, 671 w, 578 w, 548 w, 522 m, 466 m, 416 w. UV–Vis (DMSO, λ (nm)): 300.

4.3.5. Synthesis of [Zn (valp)$_2$(2-ampic)$_2$] (5)

Same procedure was followed as in compound **2** except that oily product was formed after evaporation. This oily product was washed with ether to form solid. The stoichiometry of the reaction was 2-ampic (0.62 g, 5.7 mmol) and complex (**1**) (1.00 g, 1.4 mmol). The compound is soluble in methanol, ethanol, chloroform and acetone.

$[Zn(valp)_2(2\text{-}ampic)_2]$ (**5**): 80% (1.27 g) yield, m.p. (98–103) °C. ^{1}H NMR ($CDCl_3$): δ (ppm) 0.84 (t, 6H, $CH_{3(valp)}$, $^3J_{H\text{-}H}$ = 7.1 Hz), 1.19–1.36 (m, 6H, CH_2), 1.52 (m, 2H, CH_2), 2.33 (m, 1H, $CH_{(valp)}$), 2.37 (s, 3H, CH_3), 5.00 (bs, 2H, NH_2), 6.30 (d, 1H, CH, $^3J_{H\text{-}H}$ = 8.4 Hz), 6.46 (d, 1H, CH, $^3J_{H\text{-}H}$ = 7.5 Hz), 7.31 (t, 1H, CH, $^3J_{H\text{-}H}$ = 7.5 Hz). ^{13}C{^{1}H} NMR ($CDCl_3$): δ (ppm) 14.39 ($CH_{3(valp)}$), 20.93 (CH_2), 23.84 (CH_3), 35.42 (CH_2), 47.65 ($CH_{(valp)}$), 106.43 (CH), 113.20 (CH), 138.90 (CH), 156.12 (**C**–CH_3), 158.33 (C–NH_2). IR (KBr, cm^{-1}): 3315 s, 3162 s, 2956 s, 2930 s, 2870 m, 1679 s, 1616 vs, 1567 s, 1494 s, 1442 m, 1384 s, 1352 m, 1300 w, 1223 m, 1168 m, 1115 s, 1066 w, 1005 s, 934 m, 860 m, 782 s, 757 m, 670 m, 578 m, 569 w, 540 w, 500 m, 430 w. UV–Vis (DMSO, λ (nm)): 300.

4.4. X-ray crystallography

X-ray intensities data of complexes **2**, **3** and **4** were carried out at room temperature on a Bruker SMART APEX CCD X-ray diffractometer system (graphite–monochromated Mo Kα radiation λ = 0.71073 Å) by using the SMART software package [109]. The data were reduced and integrated by the SAINT program package [110]. The structure was solved and refined by the SHELXTL software package [111]. H atoms were located geometrically and treated with a riding model. Crystal data and details of the data collection and refinement are summarized in Table 9.

4.5. Anti-bacterial activity

Three Gram-positive bacteria (*M. luteus*, *S. aureus*, and *B. subtilis*) and three Gram-negative bacteria (*E. coli*, *K. pneumonia* and *P. mirabilis*), were used to test the compounds anti-bacterial activity. The tests were carried out using the agar-well diffusion method [112]. Single bacterial colonies were dissolved in sterile saline until the suspended cells reached the turbidity of McFarland 0.5 Standard. The bacterial inocula were spread on the surface of the nutrient agar with help of a sterile cotton swab and wells (6 mm in diameter), were dug in the media with the help of sterile glassy borer. 50 μL of the recommended concentration of the test samples (10 mmol/L in DMSO) were added in the respective wells. Another well supplemented with DMSO served as negative control. The plates were incubated immediately at 37 °C for 24 h. The anti-bacterial activity was determined by measuring the diameter of the zone of complete growth inhibition in millimeter (mm). The results are the average of three trials and they stated as average ± standard deviation.

Three complexes **1**, **2** and **3** were selected for further antibacterial studies. Serial dilutions of these complexes and their parent ligands were prepared (in DMSO) to achieve decreasing concentrations ranging between 10 mmol/L and 0.2 mmol/L. All the dilutions of each complex and its parent ligand were tested in the same plate using the same procedure. Two sets of data have been recorded the inhibition zone diameter (IZD) at 10, 5 and 2.5 mmol/L concentrations, and the minimum inhibition concentration (MIC) for the complexes and their parent ligands.

4.6. .Anti-malarial activity

4.6.1. In vitro testing for anti-malarial activity using semi-quantitative method

According to Deharo et al. [27]. a mixture containing of 50 μL of (0.5 mg/ml) hemin chloride freshly dissolved in dimethylsulphoxide (DMSO), 100 μL of (0.5 M) sodium acetate buffer (pH 4.4), and 50 μL of different concentrations of the complex dissolved in pure water, was incubated in a normal non-sterile 96-well flat bottom plate at 37 °C for 18–24 h. It is important that the solutions be added to the plate in this order-. The plate was then centrifuged for 10 min at 4000 rpm. The supernatant was removed and the pH of reaction was measured. The final pH of the mixture should be between (5.0–5.2). The wells were washed with 200 μL DMSO per well to remove free hemin chloride. The plate was centrifuged again, discarding the supernatant afterward. The residual β-hematin was then dissolved in 200 μL of 0.1 M NaOH to form an FP that can be measured spectrophotometrically. Finally the

absorbance was read at 405 nm using ELISA reader Note, ultra pure water was used as negative control; meanwhile chloroquine dissolved in ultra-pure water was used as positive control.

4.6.2. Quantitative test

According to Blauer and Akkawi [24] Freshly prepared stock solution of hemin chloride was prepared by dissolving the salt in dimethysulfoxide (DMSO) and incubated for 30 min at 30 °C; stock solution of the complex used was prepared using DMSO. (0.5 M) sodium acetate buffer (pH 4.4) was also prepared, the final concentration of hemin and the complex in the reaction were 0.2 and 0.4 mM respectively, The whole mixture was left for 18–24 h at 37 °C without stirring. The total volume of the reaction mixture was 32 mL, and the final pH was 4.9–5.2.

Samples were centrifuged for 10 min using a serological (Jouan B4) centrifuge. The supernatant was discarded and the precipitate was washed with DMSO and quantitatively transferred to a Millipore Swinnex 13 filter containing Whatman filter paper No. 50, already lyophilized to a constant weight in freeze-drying machine (Labconco Freezone). DMSO was passed slowly through the filter until the filtrate remained feebly colored and washed again with ultra-pure water. The remaining was then lyophilized to a constant weight.

Acknowledgment

The authors thank the office of Vice President for Academic Affairs at Birzeit University for their financial support.

Appendix A. Supplementary material

CCDC 900563 (**2**), CCDC 908412 (**3**) and CCDC 900564 (**4**) contain the supplementary crystallographic data for this paper. These data can be obtained free of charge from the Cambridge Crystallographic Data Centre via www.ccdc.cam.ac.uk/data_request/cif.

Appendix B. Supplementary data

Supplementary data related to this article can be found at http://dx.doi.org/10.1016/j.ejmech.2014.01.067.

References

[1] R.R. Chrichton, Biological Inorganic Chemistry: An Introduction, Elsevier, Oxford, 2008.
[2] I. Bertini, F. Briganti, A. Scozzafava, Zinc proteins, in: G. Berthon (Ed.), Handbook of Metal–Ligand Interaction in Biological Fluids: Bioinorganic Chemistry, vol. 1, Marcel Dekker, New York, 1995, pp. 175–191.
[3] A.S. Parasad, Functional roles of zinc, in: G. Berthon (Ed.), Handbook of Metal–Ligand Interactions in Biological Fluids: Bioinorganic Medicine, Marcel Dekker, New York, 1995, pp. 232–243.
[4] D.K. Blencowe, A.P. Morby, FEMS Microbiol. Rev. 27 (2003) 291–311.
[5] J. Yao, Y. Liu, H.G. Liang, C. Zhang, J.Z. Zhu, X. Qin, M. Sun, S.S. Qu, Z.N. Yu, J. Therm. Anal. Calorim. 79 (2005) 39–43.
[6] S. Atmaca, K. Gul, R. Cicek, Turk. J. Med. Sci. 28 (1998) 595–597.
[7] Z.Q. Li, F.J. Wu, Y. Gong, C.W. Hu, Y.H. Zhang, M.Y. Gan, Chin. J. Chem. 25 (2007) 1809–1814.
[8] S.H. Auda, I. Knutter, B. Bretschneider, M. Bransch, Y. Mrestani, C. Crobe, R.H.H. Neubert, Pharmaceuticals 2 (2009) 184–193.
[9] D. Rathore, Strategies for malaria control, in: vbi scientific annual report, 2006, pp. 49–53.
[10] WHO, World Malaria Report, World Health Organization, 2012.
[11] J. Liu, I. Gluzman, M.E. Drew, D.E. Goldberg, J. Biol. Chem. 280 (2005) 1432–1437.
[12] R. Banerjee, J. Liu, W. Beatty, L. Pelosof, M. Klemba, D.E. Goldberg, Proc. Natl. Acad. Sci. USA 99 (2002) 990–995.
[13] P.J. Rosenthal, Int. J. Parasitol. 34 (2004) 1489–1499.
[14] D.G. Spiller, P.G. Bray, R.H. Hughes, S.A. Ward, M.R.H. White, Trends Parasitol. 18 (2002) 441–444.
[15] S. Pagola, P.W. Stephens, D.S. Bohle, A.D. Kosar, S.K. Madsen, Nature 404 (2000) 307–310.
[16] A.F.G. Slater, W.J. Swiggard, B.R. Orton, W.D. Flitter, D.E. Goldberg, A. Cerami, G.B. Henderso, Proc. Natl. Acad. Sci. USA 88 (1991) 325–329.
[17] D. Goldberg, A. Slater, A. Cerami, G. Henderson, Proc. Natl. Acad. Sci. (USA) 87 (1990) 931–935.
[18] T.J. Egan, J.M. . Combrinck, J. . Egan, G.R. . Hearne, H.M. . Marques, S. . Ntenteni, B.T. . Sewells, P.J. . Smith, D. . Taylor, D.A. . Vanschalkwyk, J.C. . Walden, Biochem. J. 365 (2002) 343–347.
[19] M. Oliveira, S. Kycia, A. Gomez, A. Kosar, D. Bohle, E. Hempelmann, D. Menezes, M. Vannier-Santos, P. Oliveira, S. Ferreira, FEBS Lett. 579 (2005) 6010–6016.
[20] A.V. Pandey, V.K. Babbarwal, J.N. Okoyeh, R.M. Joshi, S.K. Puri, R.L. Singh, V.S. Chauhan, Biochem. Biophys. Res. Commun. 308 (2003) 736–743.
[21] J. David Sullivan Jr., Hemozoin: a Biocrystal Synthesized during the Degradation of Hemoglobin, vol. 9, The Malaria Research Institute, Johns Hopkins University, 2000, pp. 129–137.
[22] G. Blauer, M. Akkawi, Biochem. J. 346 (2000) 249–250.
[23] G. Blauer, M. Akkawi, Arch. Biochem. Biophys. 398 (2002) 7–11.
[24] G. Blauer, M. Akkawi, J. Inorg. Biochem. 66 (1997) 145–152.
[25] T.E. Wellems1, C.V. Plowe, J. Infect. Dis. 184 (2001) 770–776.
[26] K.L. Waller, R.A. Muhle, L.M. Ursos, P. Horrocks, D. Verdier-Pinard, A.B.S. Sidhu, H. Fujioka, P.D. Roepe, D.A. Fidock, J. Biol. Chem. 278 (2003) 33593–33601.
[27] E. Deharo, R.N. Garcia, P. Oporto, A. Gimenez, M. Sauvian, V. Jullian, H. Ginsburg, Exp. Parasitol. 100 (2002) 252–256.
[28] S.B.R. Fagundes, Rev. Neurocienc. 16 (2008) 130–136.
[29] W.H. Feng, S.C. Kenney, Cancer Res. 66 (2006) 8762–8769.
[30] R.A. Blaheta, H. Nau, M. Michaelis, J. Ciantl Jr., Curr. Med. Chem. 9 (2002) 1417–1433.
[31] N. Esiobu, N. Hoosein, Antonie Leeuwenhoek 83 (2003) 63–68.
[32] A.L. Abuhijleh, Polyhedron 15 (1996) 285–293.
[33] A.L. Abuhijleh, C. Woods, J. Inorg. Biochem. 64 (1996) 55–67.
[34] A.L. Abuhijleh, C. Woods, Inorg. Chim. Acta 209 (1993) 187–193.
[35] A.L. Abuhijleh, J. Inorg. Biochem. 68 (1997) 167–175.
[36] M.S. Veitia, F. Dumas, G. Morgant, J.R.J. Sorenson, Y. Frapart, A. Tomas, Biochimie 91 (2009) 1286–1293.
[37] P.C. Christidis, P.J. Rentzeperis, M.P. Sigalas, C.C. Hadjikostas, Z. Crystallogr. 176 (1986) 103–112.
[38] C.C. Hadjikostas, G.A. Katsoulos, M.P. Sigalas, A. Tsipis, Inorg. Chim. Acta 167 (1990) 165–169.
[39] A.L. Abuhijleh, H. Abu Ali, A.H. Emwas, J. Org. Chem. 694 (2009) 3590–3596.
[40] D.M. Griffith, B. Duff, K.H. Suponitsky, K. Kavanagh, M.P. Morgan, D. Egan, C.J. Marmion, J. Inorg. Biochem. 105 (2011) 793–799.
[41] H.M. Butter, A. Hurse, E. Thursky, A. Shulman, Aust. J. Exp. Biol. Med. Sci. 47 (1969) 541–552.
[42] F.P. Dwyer, F.I.K. Reid, Aust. J. Exp. Biol. Med. Sci. 47 (1969) 203–218.
[43] M.N. Patel, P.A. Parmer, O.S. Gandhi, V.R. Thakkar, J. Enzyme Inhib. Med. Chem. 26 (2011) 359–366.
[44] M.A. Zoroddu, S. Zanetti, R. Pogni, R. Basosi, J. Inorg. Biochem. 63 (1996) 291–300.
[45] M.O. Agwara, P.T. Ndifon, N.B. Ndosiri, A.G. Poboudam, D.M. Yufanyi, A. Mohamadou, Bull. Chem. Soc. Ethiop. 24 (2010) 383–389.
[46] N. Raman, R. Jeyamurugan, A. Sakthivel, R. Antony, J. Iran. Chem. Res. 2 (2009) 277–291.
[47] A. Bolhuis, L. Hand, J. Marshall, A.D. Richards, A. Rodger, J. Aldrich-Wright, Eur. J. Pharm. Sci. 42 (2011) 313–317.
[48] T. Suksrichavalit, S. Prachayasittikul, C. Nantasenamat, C. Isarankura-na-ayudhya, V. Prachayasittikul, Eur. J. Med. Chem. 44 (2009) 3259–3265.
[49] A.T. Colak, F. Colak, O.Z. Yesilel, D. Akduman, F. Yilmaz, M. Tumer, Inorg. Chim. Acta 363 (2010) 2149–2162.
[50] J.A. Oballeye, A.C. Tella, R.O. Aris, Adv. Nat. Appl. Sci. 3 (2009) 43–48.
[51] R.N. Patel, N. Singh, K.K. Shukla, U.K. Chauhan, J. Niclos-Gutierrez, A. Castineiras, Inorg. Chim. Acta 357 (2004) 2469–2475.
[52] D.O. White, A.W. Harris, Aust. J. Exp. Biol. 41 (1963) 517–526.
[53] A. Shulman, D.O. White, Chem.-Biol. Interact. 6 (1973) 407–413.
[54] F. Dumitrascu, M.R. Caira, C. Draghici, M.T. Caproiu, L. Barbu, E. Miu, Rev. Roum. Chim. 53 (2008) 183–187.
[55] A. Mohindru, J.M. Fisher, M. Rabinovitz, Biochem. Pharmacol. 32 (1983) 3627–3632.
[56] A. Shulman, G.M. Laycock, Chem.-Biol. Interact. 16 (1977) 89–99.
[57] N. Margiotta, G. Natile, F. Capitelli, F.P. Fanizzi, A. Boccarelli, P. de Rindalis, D. Giordano, M. Coluccia, J. Inorg. Biochem. 100 (2006) 1849–1857.
[58] E. Szunyogova, D. Mudronovo, K. Gyoryova, R. Nemcova, J. Kovarova, L. Pkanova-Findorakova, J. Therm. Anal. Calorim. 88 (2007) 355–361.
[59] E. Szunyogova, K. Gyoryova, D. Hudecova, L. Piknova, J. Chomic, Z. Vargova, V. Zelenak, J. Therm. Anal. Calorim. 88 (2007) 219–223.
[60] K. Gyoryova, E. Szunyogova, J. Kovarova, D. Hudecova, D. Mudronova, E. Juhaszova, J. Therm. Anal. Calorim. 72 (2003) 587–596.
[61] K. Gyoryova, J. Kovarova, E. Andogova, V. Zelenak, F.A. Nour El-Dean, J. Therm. Anal. Calorim. 67 (2002) 119–128.
[62] V. Zelenak, K. Gyoryova, D. Mlynarcik, Met.-Based Drugs 8 (2002) 269–274.
[63] E. Andogova, K. Gyoryova, F.A. Nour Al-Dien, J. Therm. Anal. Calorim. 69 (2002) 245–253.
[64] K. Gyoryova, V. Balek, V. Zelenak, Thermochim. Acta 234 (1994) 221–232.
[66] P. Lemoine, B. Viossat, N.H. Dung, A. Tomas, G. Morgant, F.T. Greenaway, J.R.J. Sorenson, J. Inorg. Biochem. 98 (2004) 1734–1749.

[67] C.S. Lai, E.R.T. Tiekink, Appl. Organomet. Chem. 17 (2003) 255–256.
[68] V. Viossat, P. Lemoine, E. Dayan, N.H. Dung, B. Viossat, J. Mol. Struct. 741 (2005) 45–52.
[69] A.J. Pallenberg, T.M. Morschner, D.M. Barnhart, Polyhedron 16 (1997) 2711–2719.
[70] M. Harvey, S. Baggio, R. Baggio, A.W. Mombru, Acta. Crystallogr. C55 (1999) 308–310.
[71] Y.M. Lee, S.K. Kang, G. Chung, Y.K. Kim, S.Y. Won, Choi, J. Coord. Chem. 56 (2003) 635–646.
[72] O. Yar, L. Lessinger, Acta. Crystallogr. C51 (1995) 2282–2285.
[73] B. Jasiewicz, W. Boczon, T. Borowiak, I. Wolska, J. Mol. Struct. 875 (2008) 152–159.
[74] A. Pienaar, Ph.D Thesis: Metal Carboxylate Complexes Relevant to the Fischer–Tropsch Synthesis, University of Stellenbosch, Stellenbosch, 2005.
[75] R.K. Hocking, T.W. Hambley, Inorg. Chem. 42 (2003) 2833–2835.
[76] A.W. Addison, T.N. Rao, J. Chem. Soc. Dalt. Trans. (1984) 1349–1356.
[77] S.I. Vagin, A.K. Ott, B. Rieger, Chem. Ing. Tech. 79 (2007) 767–780.
[78] W. Clegg, I.R. Little, B.P. Straughan, J. Chem. Soc. Dalt. Trans. (1986) 1283–1288.
[79] Y. Gui, D. Long, W. Chen, J. Huang, Acta. Crystallogr. C54 (1998) 1605–1607.
[80] Q. Zhou, T.W. Hampley, B.J. Kennedy, P.A. Lay, P. Turner, B. Warwick, J.R. Biffin, H.L. . Regtop, Inorg. Chem. 39 (2000) 3742–3748.
[81] V. Zelenak, M. Sabo, W. Massa, J. Cernak, Acta. Crystallogr. C60 (2004) m85–m87.
[82] W. Clegg, P.A. Hunt, B.P. Straughan, Acta. Crystallogr. C51 (1995) 613–617.
[83] B. Singh, J.R. Long, F.F. de Biani, D. Gatteschi, P. Stavropoulos, J. Am. Chem. Soc. 119 (1997) 7030–7047.
[84] Y.B. Koh, G.G. Christoph, Inorg. Chem. 18 (1979) 1122–1128.
[85] P. Ren, N.P. Su, J.G. Qin, M.W. Day, C.T. Chen, Chin. J. Struct. Chem. 21 (2002) 38–41.
[86] J. Qin, N. Su, C. Dai, C. Yang, D. Liu, M.W. Day, B. Wu, C. Chen, Polyhedron 18 (1999) 3461–3464.
[87] L. Mei, T.H. Ming, L.Q. Rong, S. Jie, Y.S. Zhong, L.X. Liang, J. Chem. Sci. 121 (2009) 435–440.
[88] W.D. Horrocks, J.Y. Ishley, R.R. Whittle, Inorg. Chem. 21 (1982) 3265–3269.
[89] S.S.S. Raj, H.K. Fun, P.S. Zhao, F.F. Jian, L.D. Lu, X.J. Yang, X. Wang, Acta. Crystallogr. C56 (2000) 742–743.
[90] D. Rishmawi, J. Kelley, M.D. Smith, L. Peterson, H.C. zur Loy, Acta. Crystallogr. E65 (2009) m331.
[91] G.B. Deacon, R.J. Philips, Coord. Chem. Rev. 33 (1980) 227–250.
[92] K. NaKamoto, Infrared and Raman Spectra of Inorganic and Coordination Compounds: Part B, John Wiley and Sons, New Jersey, 2009.
[93] V. Zelenak, Z. Vargova, K. Gyoryova, Spectrochim. Acta Part A 66 (2007) 262–272.
[94] F. Gao, P. Yang, J. Xie, H. Wang, J. Inorg. Biochem. 60 (1995) 61–67.
[95] W. Ferenc, B. Cristovao, J. Sarzynski, J. Therm. Anal. Calorim. 86 (2006) 783–789.
[96] L. Findorakova, K. Gyoryova, J. Kovarova, V. Balek, F.A. Nour El-Dien, L. Halas, J. Therm. Anal. Calorim. 95 (2009) 923–928.
[97] M.L. Niven, G.C. Percy, Transit. Met. Chem. 3 (1978) 267–271.
[98] Z.H. Cohan, C.T. Supuran, A.J. Scozzafava, Enzyme Inhib. Med. Chem. 19 (2004) 79–84.
[99] S. Dinkov, M. Arnaudov, Spectrosc. Lett. 32 (1999) 165–180.
[100] B.H. Ye, X.Y. Li, I.D. Williams, X.M. Chen, Inorg. Chem. 41 (2002) 6426–6431.
[101] S.J. Lin, T.N. Hong, J.Y. Tung, J.H. Chen, Inorg. Chem. 36 (1997) 3886–3891.
[102] D.K. Lavallee, J.D. Doi, Inorg. Chem. 20 (1981) 3345–3349.
[103] D.K. Lavallee, M.D. Baughman, M.P. Philips, J. Am. Chem. Soc. 99 (1977) 718–724.
[104] J.E. Figard, J.V. Paukstelis, E.F. Byrne, J.D. Petersen, J. Am. Chem. Soc. 99 (1977) 8417–8425.
[105] Z. Derikvand, G.R. Talei, H. Aghabozorg, M.M. Olmstead, A. Azadbakht, A. Nemati, J.A. Gharamaleki, Chin. J. Chem. 28 (2010) 2167–2173.
[106] F.P. Prunchnik, M. Bien, T. Lachowicz, Met. Based Drugs 3 (1996) 185–195.
[107] H. Abu Ali, M.D. Darawsheh, E. Rappocciolo, Polyhedron 61 (2013) 235–241.
[108] I. Weissbuch, L. Leiserowitz, Chem. Rev. 108 (2008) 4899–4914.
[109] SMART-NT V5.6, Bruker AXS GMBH, D-76181 Karlsruhe, Germany, 2002.
[110] SAINT-NT V5.0, BRUKER AXS GMBH, D-76181 Karlsruhe, Germany, 2002.
[111] SHELXTL-NT V6.1, BRUKER AXS GMBH, D-76181 Karlsruhe, Germany, 2002.
[112] M.I. Atta-ur-Rahman, W.J. Thomson Choudhary, Bioassay Techniques for Drug Development, Harwood Academic, The Netherlands, 2001.